Proceedings of the Institute of Acoustics

ACOUSTIC NONLINEARITY PARAMETERS AND HIGHER-ORDER ELASTIC CONSTANTS OF CRYSTALS

John H. Cantrell*

Cavendish Laboratory, University of Cambridge, Madingley Rd., Cambridge CB3 OHE

ABSTRACT

A quantitative measure of elastic wave nonlinearity in crystals is provided by the acoustic nonlinearity parameters. It is shown that the magnitudes of the nonlinearity parameters strongly depend on the crystalline structure of the solid and that the dependence for many structures is dominated by the ionic core-core repulsive exchange interactions of neighbouring atoms. Measurements of the nonlinearity parameters are used to calculate the Born-Mayer "hardness" parameters for several crystals of cubic symmetry. The measurements are in good agreement with values of the parameters determined from other methods. The Born-Mayer parameters together with sound velocity measurements are then used to calculate the elastic constants of orders two through five for the crystals. It is found that the magnitude of the elastic constants of each order is approximately a factor of ten larger than the magnitude of the previous order and is opposite in sign.

INTRODUCTION

The acoustic nonlinearity parameters are found to play an increasingly prominent role in describing the thermoelastic properties of crystalline solids since they directly quantify the anharmonic character of the lattice modes. The parameters appear, for example, in the thermodynamic state functions[1], in equations describing the thermal expansivity of solids[2], and in expressions for the temperature dependence of elastic moduli[3]. They appear as scaling parameters in the equations for the acoustic radiation stress[4] and radiation-induced static strains[5,6]. They are also found to be strongly correlated with Brinell hardness numbers for metallic alloys[7,8].

We define the acoustic nonlinearity parameters from their appearance in the elastic wave equations. For a lossless solid of arbitrary crystalline symmetry the nonlinear equations of motion in Lagrangian coordinates are[9] (Einstein summation convention)

$$\rho_o \frac{\partial^2 u_i}{\partial t^2} = \left[C_{ijkl} + (C_{jlmn}\delta_{ik} + C_{ijnl}\delta_{km} + C_{jknl}\delta_{im} + C_{ijklmn})\frac{\partial u_m}{\partial a_n} \right] \frac{\partial^2 u_k}{\partial a_j \partial a_l} \qquad (1)$$

where u_i are Cartesian components of the wave displacement vector (particle displacement), a_i are Lagrangian coordinates, ρ_o the unperturbed mass density, t is time, and δ_{ij} are Kronecker deltas. The Brugger elastic constants $C^{(n)}_{ijklmn..}$ of order n are defined from the internal energy per unit mass U as [10]

$$C^{(n)}_{ijklmn...} = \rho_o \left(\frac{\partial^n U}{\partial \eta_{ij} \partial \eta_{kl} \partial \eta_{mn} \cdots} \right)_{\eta=0} \qquad (2)$$

where η_{ij} are the Langrangian strains.

We assume that an initially sinusoidal wave of amplitude A, unit polarization w, and angular frequency ω is launched from a planar surface such that the boundary condition

$$u_i = Aw_i \cos \omega t \quad , \qquad k_j a_j = kl = o \tag{3}$$

is satisfied. In Eq.(3) k is the propagation vector and l is the propagation distance from the planar surface. The self-resonant solution to Eq.(1) subject to the boundary condition, Eq.(3), is [9]

$$u_i = \frac{1}{8}\beta k^2 A^2 l w_i + Aw_i \cos(\omega t - k_j a_j) - \frac{1}{8}\beta k^2 A^2 l w_i \cos(2\omega t - 2k_j a_j) + \ldots \tag{4}$$

where the acoustic nonlinearity parameter β is defined by

$$\beta = -\frac{(C_{jlpq}\delta_{ik} + C_{ijql}\delta_{kp} + C_{jkql}\delta_{ip} + C_{ijklpq})\, N_j N_l N_q w_i w_k w_p}{C_{ijkp} N_j N_i w_i w_k}, \quad N = \frac{k}{k}. \tag{5}$$

The static term on the right-hand side of Eq.(4) was not originally included in the solution of ref. 9. The relevance of the static term and its relationship to the acoustic radiation stress is discussed in ref. 6. We see from Eq.(4) that the nonlinearity parameters prominently appear in both the static and harmonic generation terms. The β parameters can be determined directly from absolute amplitude measurements of the acoustic waveform[5,6,11] or calculated from Eq.(5) with knowledge of the second and third-order elastic constants obtained from other measurement techniques[12].

CRYSTALLINE STRUCTURE DEPENDENCE OF NONLINEARITY PARAMETERS

Experimental elastic data on 29 crystals of cubic symmetry were obtained from the literature. The nonlinearity parameters along the pure mode propagation directions [100], [110], and [111] were either calculated from Eq.(5) or recorded from direct β measurements. The results for NaCl-structured crystals are given in Table I for wave propagation along the [100] direction. We see that the values of the nonlinearity parameters are bound between 14.0 and 15.4, a variation of approximately 10 percent. The values of the elastic constants for these crystals, however, vary by several hundred percent. Similar results are found for crystals of other structures and are summarized in Table II (again for wave propagation along [100]). We list in the table the structure of the cubic crystal, the type of atomic bonding, the range of values of β for all crystals having a given structure, and the average of the β's in that range. We see that the acoustic nonlinearity parameters are strongly ordered according to the type of crystalline structure. The range of values of β for a given structure is distinct; overlap of ranges occur only slightly for fcc and fluorite structures.

Table I. Longitudinal mode acoustic nonlinearity parameters β along [100] for NaCl-structured crystals.

Solid:	RbBr	LiBr	RbI	NaCl	KCl	LiF	MgO	RbCl	NaF
Bonding:	Ionic	Ionic	Ionic	Ionic	Ionic	Ionic	Ionic	Ionic	Ionic
β[100]:	15.4	15.2	15.0	14.6	14.4	14.2	14.1	14.0	14.0

Table II. Comparison of Structure, Bonding, and Acoustic Nonlinearity Parameters Along [100] Direction of Cubic Crystals.

Structure	Bonding	β_{av}	Range of β
NaCl	Ionic	14.6	14.0-15.4
BCC	Metallic	8.2	7.4 - 8.8
FCC (inert gas)	Van der Waals	6.4	5.8 - 7.0
FCC	Metallic	5.6	4.0 - 7.0
Fluorite	Ionic	3.8	3.4 - 4.6
Zincblende	Covalent	2.2	1.8 - 3.0

The influence of the type of atomic bonding may be inferred from a comparison of fcc-structure crystals. The β's for the fcc metallic-bonded crystals and the fcc Van der Waals-bonded crystals are approximately equal even though the difference in strength of these bonds is very large. We thus infer that the influence of the bonding on the value of the nonlinearity parameter is small compared to that of the crystalline structure.

THEORETICAL MODEL

The experimentally determined structure dependence of the nonlinearity parameters suggests that the geometry of the local atomic arrangement and perhaps shape, but not strength, of the interatomic potential are dominant factors in determining the magnitude of β. This suggests in turn a model based in first-order approximation on a short-range, two-body, central-force potential. We follow an approach originally suggested by Wigner and Seitz[13] and used extensively by other researchers.[13-16] We consider only the static lattice contributions to the internal energy and write the potential energy density of the static lattice as

$$\rho_o U = \frac{1}{2V_o} \Sigma \phi(r) \qquad (6)$$

where $\phi(r)$ is the energy per ion as a function of ion pair separation r, the sum is taken over ion pairs, and V_o is the atomic volume.

The relationship between the Lagrangian strains and the ion pair separation is[17]

$$r^2 - r_o^2 = 2 \Sigma \xi_i \xi_j \eta_{ij} \tag{7}$$

where r_o is the initial (undeformed) two-particle separation distance, r is the final (deformed) two-particle separation distance, and ξ_i is the difference in Cartesian coordinates of the two particles in the initial state. From Eq.(7) we obtain

$$\frac{\partial}{\partial \eta_{ij}} = \xi_i \xi_j \frac{1}{r} \frac{d}{dr} = \xi_i \xi_j D . \tag{8}$$

From Eqs.(2), (6), and (8) we get, for nearest neighbour interactions only, that

$$C^{(n)}_{ijklmn...} = \frac{1}{2V_o} \Sigma (\xi_i \xi_j \xi_k \xi_l \xi_m \xi_n ....) [D^n \phi(r)]_{r = r_o} \tag{9}$$

From Eq.(9) we may write

$$C^{(2)}_{11} = \frac{1}{2V_o} \Sigma \xi_1^4 [D^2 \phi (r)]_{r = r_o} \tag{10a}$$

$$C^{(3)}_{111} = \frac{1}{2V_o} \Sigma \xi_1^6 [D^3 \phi (r)]_{r = r_o} \tag{10b}$$

where we have used Voigt contraction of the indices (subscripts) for the elastic constants.

For acoustic waves propagating along the [100] direction in cubic crystals we find from Eqs.(5) and (10) that the nonlinearity parameters are given by

$$\beta = - [3 + \frac{\Sigma \xi_1^6 [D^3 \phi(r)]_{r=r_o}}{\Sigma \xi_1^4 [D^2 \phi(r)]_{r=r_o}}] \tag{11}$$

The crystalline structure dependence of β enters through ξ_1 and the summation.

We now introduce as the central force potential the Born-Mayer potential written in the form suggested by Hiki and Granato[15]

$$\phi(r) = A e^{-B(r/r_o - 1)} \tag{12}$$

where r_o represents the equilibrium separation of nearest neighbour atoms and B is the "hardness" parameter. This potential provides an excellent representation of the quantum mechanical exchange interaction between closed-shell ionic cores of neighbouring atoms.

From Eqs.(11)-(12) and knowledge of the atomic arrangement we obtain the relationship between the Born-Mayer hardness parameter B and the acoustic nonlinearity parameters along the [100] direction for cubic crystals (i.e. cubic Bravais lattice) having three different structures (i.e. bases). Summing over nearest neighbours only, we find for face-centered cubic (fcc) crystals

$$B(fcc) = \frac{1}{2} [(3 + 2\beta) + [(3 + 2\beta)^2 + 4(3 + 2\beta)]^{1/2}] \tag{13}$$

for body-centered cubic (bcc) and cesium chloride (CsCl) structured crystals

$$B(bcc,CsCl) = \frac{1}{2}\{(6 + 2\beta) + [(6 + 3\beta)^2 + 4(6 + 3\beta)]^{1/2}\} \quad (14)$$

and for NaCl-structured crystals

$$B(NaCl) = \frac{1}{2}\{\beta + [\beta^2 + 4\beta]^{1/2}\} . \quad (15)$$

COMPARISON OF BORN-MAYER PARAMETERS

From Eqs.(13)-(15) and experimental values of the nonlinearity parameters we may calculate the Born-Mayer B parameters. Table III shows a comparison between the Born-Mayer parameters so calculated and literature value of B obtained from other methods (e.g. neutron scattering). We see that agreement between the present and other determinations for fcc and CsCl-structured crystals is very good and indicates that the short range Born-Mayer potential makes the dominant contribution to the nonlinearity parameters of the solids. For NaCl-structured crystals, however, the values of B determined from β measurements is approximately 50 per cent greater than the literature values. The reason for this discrepancy is that these solids have a relatively strong spatial rate of change of electrostatic potential which makes a contribution to β comparable to that of the Born-Mayer term in Eq.(11). The dominating spatial rate of change of the Born-Mayer potential for fcc and CsCl-structured crystals, however, becomes even more dominating as the order of the spatial derivative increases. This suggests according to Eq.(9) that use of the Born-Mayer potential to calculate the elastic constants becomes more accurate for these structures as the order of the elastic constants so calculated increases.

Table III. Comparison of Present Calculation of the Born-Mayer Parameter B with other Determinations

Crystal	Structure	B (present work)	B (other work)
Cu	fcc	13.2	13.0[a]
Ag	fcc	11.7	12.8-13.8[b]
Au	fcc	15.9	14.4[c]
β-brass	CsCl	28.3	29.3[d]
NaCl	NaCl	15.5	9.8[e]
RbI	NaCl	15.9	12.4[e]
Kcl	NaCl	15.3	10.1[e]

[a] J.B. Gibson, A.N. Golad, M. Milgram, and G.H. Vinegard, Phys. Rev. **120**, 1229 (1960)
[b] E. Mann and A. Seeger, J. Phys. Chem. Solids **12**, 314 (1960)
[c] M.W. Thompson, AERE Harwell, Report No. AERE-R-4694, 1964
[d] G. Gilat and G. Dolling, Phys. Rev. **138**, A1053 (1965)
[e] P.B. Ghate, Phys. Rev. **139**, A1666 (1965)

HIGH-ORDER ELASTIC CONSTANTS

Values of the second and third-order elastic constants are frequently reported in the literature. Fourth-order elastic constants have been reported only rarely while values of the fifth and high-order constants have not been reported at all. The results presented above suggest that we may calculate the elastic constants of any order n from values obtained for the previous order (n-1) according to the expression

$$\frac{C^{(n)}_{ijklmn....}}{C^{(n-1)}_{ijklmn...}} = \frac{\Sigma(\xi_i\xi_j\xi_k\xi_l\xi_m\xi_n...)[D^n\phi(r)]_{r=ro}}{\Sigma(\xi_i\xi_j\xi_k\xi_l\xi_m\xi_n...)[D^{n-1}\phi(r)]_{r=ro}} \qquad (16)$$

For simplicity we shall restrict the calculation here to elastic constants of the type $C^{(n)}_{111...}$ in Voigt notation. We shall also restrict the calculation to fcc crystals and again assume central-force Born-Mayer potentials. We obtain from Eqs.(12) and (16) for orders up to five the recurrence relations

$$\frac{C^{(3)}_{111}}{C^{(2)}_{11}} = -\frac{B^2 + 3B + 3}{2(B + 1)}$$

$$\frac{C^{(4)}_{1111}}{C^{(3)}_{111}} = -\frac{B^3 + 6B^2 + 15B + 15}{2(B^2 + 3B + 3)} \qquad (17)$$

$$\frac{C^{(5)}_{11111}}{C^{(4)}_{1111}} = -\frac{B^4 + 10B^3 + 45B^2 + 105B + 105}{2(B^3 + 6B^2 + 15B + 15)}$$

The Born-Mayer B parameters are again obtained from Eq.(13) together with measurements of the acoustic nonlinearity parameters β. It is clear from Eqs.(17) that all higher-order elastic constants under consideration may be calculated from knowledge of B and measurements of $C^{(2)}_{11} = \rho v$ where ρ is the mass density of the crystal and v is the sound velocity along the [100] direction. Since the Born-Mayer parameters are positive we see immediately from Eqs.(17) that the sign of the elastic constant of a given order is opposite to that of the previous order.

RESULTS AND CONCLUSIONS

Table IV shows the results of the calculations for several fcc crystals. We see that in general the magnitude of the elastic constants of each order is approximately a factor of ten larger than the magnitude of the previous order and is opposite in sign. The value of the fourth-order elastic constant calculated here for Cu is in complete agreement with the results of Garber and Granato[18] who calculated the constant from a theory based on the measured temperature dependence of the second-order elastic constants. Such agreement is surprising considering the crudeness of the approximations made in both theoretical approaches. The present calculations of the fourth-order constants of Ag and Au differ from the Garber-Granato results by approximately 30 percent, but again this is reasonable agreement. Fourth-order constants for Al have not been previously reported in the literature nor have values of the fifth-order elastic constants for any material. They are reported here for the first time. Although derivation of the complete set of independent fifth-order constants for crystals of triclinic and

the most symmetric cubic classes is to be published elsewhere, the results reported here for $C^{(5)}_{11111}$ is representative of the relative magnitudes and signs of these constants compared to that of the previous orders.

Table IV. Values of elastic constants of orders two through five obtained from present work (in units of 10^{12} dyne/cm^2).

Crystal	$C^{(2)}_{11}$	$C^{(3)}_{111}$	$C^{(4)}_{1111}$	$C^{(5)}_{11111}$
Cu	1.66	-12.7	104	-913
Ag	1.22	-8.43	63.1	-511
Au	1.93	-17.3	165	-1680
Al	1.07	-10.8	114	-1280

Finally, knowledge of the elastic constants is important in understanding the thermoelastic properties of materials and in comparing anharmonic lattice theories with experiment. The fourth and fifth-order constants in particular are found to make a considerable contribution to the stress-temperature dependence of the sound velocity[19] and calculations of these elastic constants are necessary to compare theory and experiment. The work here shows that reasonable estimates of the values of the higher-order elastic constants can be obtained from a relatively simple theory based on central-force potentials together with measurements of the acoustic velocity and nonlinearity parameters.

REFERENCES

*Permanent address: NASA Langley Research Center, Hampton, Virginia 23665-5225, U.S.A.

1. J.H. Cantrell, Ultrasonics International 1985 Conference Proceedings, (IPC Science and Technology Press Ltd., Guildford, Surrey, UK, 1985), pp.551-556.
2. J.H. Cantrell, in review.
3. J.H. Cantrell, Proceedings 1986 IEEE Ultrasonics Symposium, IEEE Cat. No. 86CH2375-4 (Institute of Electrical and Electronics Engineers, New York, 1986), pp.1079-1082.
4. J.H. Cantrell, Phys. Rev. B 30, 3214 (1984).
5. W.T. Yost and J.H. Cantrell, Phys. Rev. B 30, 3221 (1984).
6. J.H. Cantrell, W.T. Yost and P. Li, Phys. Rev. B 35, 9780 (1987).
7. P. Li, W.T. Yost, J.H. Cantrell and K. Salama, Proceedings 1985 IEEE Ultrasonics Symposium, IEEE Cat. No. 85 CH2209-5 SU (Institute of Electrical and Electronics Engineers, New York, 1985), pp.1113 - 1115.
8. H. Yang, W.T. Yost, and J.H. Cantrell, Proceedings 1987 IEEE Ultrasonics Symposium, IEEE Cat. No. 87CH2492-7 (Institute of Electrical and Electronics Engineers, New York, 1987), pp.1131 - 1135.
9. D.C. Wallace, Phys. Rev. 162, 776 (1967).
10. K. Brugger, Phys. Rev. 133, A1611 (1964).

11. See reference cited in W.T. Yost, J.H. Cantrell, and M.A. Breazeale, J. Appl. Phys. **52**, 126 (1981).
12. See references cited in R.E. Green, Jr., *Treatise on Materials Science and Technology*, Vol. 3, (Academic, New York, 1973).
13. E. Wigner and F. Seitz, Phys. Rev. **43**, 804 (1933).
14. P.B. Ghate, Phys. Rev. **139**, A1666 (1965).
15. Y. Hiki and A.V. Granato, Phys. Rev. **144**, 411 (1966).
16. R.A. Johnson, Phys. Rev. B **6**, 2094 (1972).
17. F.D. Murnaghan, *Finite Deformation of an Elastic Solid*, (Wiley, New York, 1951), p.29.
18. J.A. Garber and A.V. Granato, Phys. Rev. B **11**, 3998 (1975).
19. J.H. Cantrell, in preparation.

Proceedings of the Institute of Acoustics

PIEZOELECTRIC DETECTION OF SIGNALS IN SCANNING ELECTRON ACOUSTIC MICROSCOPY

Menglu Qian* John H. Cantrell** and F.J. Rocca

Cavendish Laboratory, University of Cambridge, Madingley Rd., Cambridge CB3 OHE

INTRODUCTION

Scanning Electron Acoustic Microscopy (SEAM) is a very useful tool for assessing near subsurface structure of materials. If the focussed electron beam in a scanning electron microscope is chopped at frequency f in the 10^5 to 10^6 Hz range the periodic heating near the irradiated region of the specimen generates an acoustic wave at the same frequency. The acoustic waves yield a scanned image signal via a transducer attached to the specimen and lock-in amplifer system. Near surface and subsurface contrast with resolution in the range 0.2μm to 10μm is produced by local variations in the thermal and elastic properties of the material as well as in electron stopping power and specimen surface topography.

The SEAM technique has two important advantages. First, it is easy to use and does not require extensive specimen preparation. More importantly, the technique provides subsurface information and delineates other specimen features not visible with images typically formed from the secondary electron signal. SEAM analysis covering various aspects of materials and device engineering [1] has become somewhat commonplace since its introduction by Brandis and Rosencwaig[2] and by Cargill [3]. But the interpretation of the image can be complicated[4,5] and is in some situations still not completely understood. The purpose of this paper is to help clarify certain contrast mechanisms in SEAM by focusing on the relationship between the output signal of the receiving piezoelectric transducer (PZT) and the thermoelastic properties of the sample. Our approach is to solve the thermal conduction equations for the sample and PZT to obtain a two-dimensional temperature distribution which is then used to solve the Navier-Stokes equation for the acoustic strain in the sample. Using the piezoelectric equations we obtain the theoretical expression of the output signal from the PZT.

TEMPERATURE DISTRIBUTION

We consider the sample-PZT system as shown in Fig. 1. The lateral dimensions of the sample and PZT are considered to be infinite. We assume that the electron beam is square-wave modulated at angular frequency ω and the thermal power density H(r,z,t) of the heat source generated by the electron beam is nominally of the form[6]:

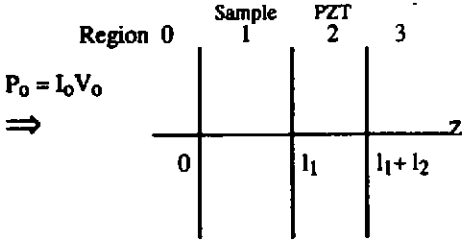

Fig. 1 Sample-PZT System

$$H(r,z,t) = (2\eta P_0\beta/\pi^2a^2)\exp(i\omega t - \beta|z-z_0| - 2r^2a^{-2}) \quad (1)$$

where η is the fraction of the primary electron beam power P_0 converted to heat power and β is the electronic attenuation coefficient. The primary beam power $P_0 = I_0V_0$ where I_0 is the beam current and V_0 is the accelerating voltage. β and z_0 are dependent on V_0 and the properties of the sample. The thermal conduction equations in the sample (Region 1) and the PZT (Region 2) are

$$\nabla^2T_1 - (1/\alpha_1)(\partial T_1/\partial t) = (-1/\kappa_1)\,H(r,z,t) \qquad \text{(Region 1)} \quad (2a)$$

$$\nabla^2T_2 - (1/\alpha_2)(\partial T_2/\partial t) = 0 \qquad \text{(Region 2)} \quad (2b)$$

where α_j is the thermal diffusivity and $j = 1,2$ represents the sample (1) or transducer (2). The thermal diffusivity and conductivity are related by the expression $\alpha_j = \kappa_j/\rho_jc_j$ where ρ_j is the mass density and C_j is the specific heat of the material.

The boundary conditions are assumed to be

$$\partial T_1(r,o,t)/\partial z = 0 \quad , \quad T_1(r,l_1,t) = T_2(r,l_1,t) \quad (3a)$$

$$\kappa_1\partial T_1(r,l_1,t)/\partial z = \kappa_2\partial T_2(r,l_1,t)/\partial z \quad , \quad \partial T_2(r,l_1+l_2,t)/\partial z = 0 \quad (3b)$$

We first write T_1 and T_2 in terms of Hankel transforms and obtain the general solution of Eq(2) as

$$T_1(r,z,t) = (e^{i\omega t}/2)\int_0^\infty [\,\Gamma(\delta)e^{-\beta|z-z_0|} + A(\delta)e^{-\sigma_1 z} + B(\delta)e^{\sigma_1 z}\,]\,J_0(\delta r)\,\delta d\delta \quad (4)$$

$$T_2(r,z,t) = (e^{i\omega t}/2)\int_0^\infty [\,C(\delta)e^{-\sigma_2(z-l_1)} + D(\delta)e^{\sigma_2(z-l_1)}\,]\,J_0(\delta r)\,\delta d\delta \quad (5)$$

where

$$A(\delta) = \{r_1e^{-\beta z_0}(d^+)_1[(b_1-1)(d^-)_2 - (b_1+1)(d^+)_2] - e^{-\beta(l_1-z_0)}[(b_1+r_1)(d^-)_2 - (b_1-r_1)(d^+)_2]\}\Gamma(\delta)/H(\delta)$$

$$B(\delta) = -\{r_1e^{-\beta z_0}(d^-)_1[(b_1+1)(d^-)_2-(b_1-1)(d^+)_2] + e^{-\beta(l_1-z_0)}[(b_1+r_1)(d^-)_2-(b_1-r_1)(d^+)_2]\}\Gamma(\delta)/H(\delta)$$

$$C(\delta) = -(d^+)_2\{e^{-\beta(l_1-z_0)}[(r_1-1)(d^-)_1 + (r_1+1)(d^+)_1] + 2r_1e^{-\beta z_0}\}\Gamma(\delta)/H(\delta)$$

$$D(\delta) = -(d^-)_2\{e^{-\beta(l_1-z_0)}[(r_1-1)(d^-)_1 + (r_1+1)(d^+)_1] + 2r_1e^{-\beta z_0}\}\Gamma(\delta)/H(\delta) \quad (6)$$

$$H(\delta) = (d^-)_1[(b_1+1)(d^-)_2 - (b_1-1)(d^+)_2] + (d^+)_1[(b_1-1)(d^-)_2 - (b_1+1)(d^+)_2]$$

and where

$$\Gamma(\delta) = \eta\beta P_o\exp(-a^2\delta^2/8)/\pi^2\kappa_1(\sigma_1^2-\beta^2), \qquad \sigma_j^2 = \delta^2 + \sigma_j'^2$$

$$\sigma_j'^2 = i\omega/\alpha_j \;, \qquad d_j^{\pm} = e^{\pm\sigma_j l_j} \;, \qquad b_1 = \kappa_2\sigma_2/\kappa_1\sigma_1 \;, \qquad r_1 = \beta/\sigma_1.$$

Using the property of Hankel transforms

$$\int_0^\infty \delta d\delta \int_0^\infty F(\delta)J_o(\delta r)rdr = F(0) \tag{6a}$$

the one-dimensional temperature distributions of the sample and PZT are given by

$$T_1(z,t) = \pi[\Gamma(o)e^{-\beta|z-z_o|} + A(o)e^{-\sigma' 1 z} + B(o)e^{\sigma' 1 z}]e^{i\omega t} \tag{4a}$$

$$T_2(z,t) = \pi[C(o)e^{-\sigma' 2(z-l_1)} + D(o)e^{\sigma' 2(z-l_1)}]e^{i\omega t} \tag{5a}$$

DISPLACEMENT DISTRIBUTION IN SAMPLE

The displacement $\mathbf{u}^{(1)}(u_r,u_z)$ at a point (r,z) in an isotropic slab of thickness l_1 will satisfy the Navier-Stokes equation:

$$\nabla^2\mathbf{u}^{(1)} + [1/(1-2\nu)]\nabla(\nabla\bullet\mathbf{u}^{(1)}) - [2(1+\nu)\rho_1/E]\partial^2\mathbf{u}^{(1)}/\partial t^2 = [2(1+\nu)\alpha_T/(1-2\nu)]\nabla T_1 \tag{7}$$

where ν is Poisson's ratio, E is Young's modulus, ρ_1 is the density of the sample, and k_1 is the elastic wave propagation number ($k_1^2 = \omega^2/c_1^2$ where $c_1^2 = E(1-\nu)/\rho_1(1+\nu)(1-2\nu)$). Using the thermoelastic potential function $\psi(r,z)e^{i\omega t}$ and the relationships between ψ and $\mathbf{u}$

$$u_r = \partial\psi/\partial r \quad , \qquad u_z = \partial\psi/\partial z \tag{8}$$

we obtain from Eqs. (7) and (8)

$$\nabla^2\Psi - [(1+\nu)/(1-\nu)]\alpha_1 T_1 + k_1^2\Psi = 0 . \tag{9}$$

The general solution of Eq.(9) is given by

$$\Psi(r,z) = [\alpha_T(1+\nu)/2(1-\nu)] \int_0^\infty [R_1(\delta)e^{-ikz_1 z} + S_1(\delta)e^{ikz_1 z} + \tag{10}$$

$$L(\delta)e^{-\beta|z-z_o|} + M(\delta)e^{-\sigma_1 z} + N(\delta)e^{\sigma_1 z}]J_o(\delta r)\delta d\delta$$

where

$$L(\delta) = \Gamma(\delta)/(\beta^2+k_1^2-\delta^2) , \qquad M(\delta) = A(\delta)/(\sigma_1^2+k_1^2-\delta^2)$$

$$N(\delta) = B(\delta)/(\sigma_1^2+k_1^2-\delta^2) , \qquad k_1^2 = \delta^2+k_{z1}^2 .$$

Therefore the two-dimensional displacement $u^{(1)}_z(r,z)$ and stress $\sigma^{(1)}_{zz}(r,z)$ in the z direction are

$$u^{(1)}_z(r,z) = [\alpha_T(1+\nu)/2(1-\nu)] \int_0^\infty \{-ik_{z1}[R_1(\delta)e^{-ik_{z1}z} - S_1(\delta)e^{ik_{z1}z}] - \quad (11)$$

$$[\beta\Gamma(\delta)e^{-\beta|z-z_0|}/(\beta^2+k_1^2-\delta^2)] - [\sigma_1[A(\delta)e^{-\sigma_1 z} - B(\delta)e^{\sigma_1 z}]/(\sigma_1^2+k_1^2-\delta^2)]\}J_0(\delta r)\delta d\delta \ , \ (z>z_0)$$

$$\sigma^{(1)}_{zz}(r,z) = [E/(1+\nu)]\{\partial u_z/\partial z + [\nu/(1-\nu)](\partial u_r/\partial r + u_r/r + \partial u_z/\partial z) - [(1+\nu)/(1-2\nu)]\alpha_T T_1\}$$

$$= [\alpha_T E/2(1-\nu)] \int_0^\infty [\delta^2-k_1^2(1-\nu)/(1-2\nu)]\{R_1(\delta)e^{-ik_{z1}z} + S_1(\delta)e^{ik_{z1}z} + \quad (12)$$

$$[\Gamma(\delta)e^{-\beta|z-z_0|}/(\beta^2+k_1^2-\delta^2)] + [A(\delta)e^{-\sigma_1 z} + B(\delta)e^{\sigma_1 z}]/(\sigma_1^2+k_1^2-\delta^2)]\}J_0(\delta r)\delta d\delta$$

From Eq. (6a) we get the one-dimensional displacement and stress

$$u^{(1)}_z(z) = [\pi\alpha_T(1+\nu)/(1-\nu)]\{-ik_1)[R_1(0)e^{-ik_1 z} - S_1(0)e^{ik_1 z}] - \quad (11a)$$

$$\beta\Gamma(0)e^{-\beta|z-z_0|}/(\beta^2+k_1^2) - \sigma_1[A(0)e^{-\sigma_1 z} - B(0)e^{\sigma_1 z}]/(\sigma_1^2+k_1^2)\} \ , \ (z > z_0)$$

$$\sigma^{(1)}_{zz}(z) = [\pi\alpha_T E k_1^2/(1-2\nu)]\{R_1(0)e^{-ik_1 z} + S_1(0)e^{ik_1 z} + \quad (12a)$$

$$[\Gamma(0)e^{-\beta|z-z_0|}/(\beta^2+k_1^2)] + [A(0)e^{-\sigma_1 z} + B(0)e^{\sigma_1 z}]/(\sigma_1^2+k_1^2)]\} \ , \ (z > z_0)$$

where $R_1(o)$ and $S_1(o)$ can be determined by boundary conditions.

DISPLACEMENT DISTRIBUTION IN PZT

If the polarization direction of the PZT disc is along the Z axis, the piezoelectric equations are given by

$$\sigma_{zz} = S^{ET}_{33}(\partial u_z/\partial z) - e^T_3 E_z - \lambda^T_3 T_2 \quad (13a)$$

$$D_z = e^T_3(\partial u_z/\partial z) + \varepsilon^{ST}_3 E_z + p^S_3 T_2 \quad (13b)$$

where S^{ET} is the compliance coefficient, e^T the piezoelectric constant, λ^T the thermo-stress constant, ε^{ST} the dielectric constant, p^S the pyroelectric constant, E_z is the component of the electric field along z, and D_z is the electric displacement along z. The temperature T_2 in the PZT is given by Eq.(5a).

From Eq(13) we get

$$\sigma^{(2)}_{zz} = S^*(\partial u^{(2)}_z/\partial z) + \lambda^* T_2 - h^* D_z \qquad (14)$$

where

$$S^* = S^{ET}_{33} + [(e^T_3)2/\epsilon^{ST}] \ , \quad \lambda^* = (e^T_3 p^S_3/\epsilon^{ST}_3) - \lambda^T_3 \quad , \quad h^* = e^T_3/\epsilon^{ST}_3 \ .$$

If there is no space charge within the PZT, as for insulating crystals or ceramics, $\mathbf{div}D = 0$ and $\partial D_z/\partial z = 0$. The equation of motion is given by

$$\rho_2(\partial^2 u^{(2)}_z/\partial t^2) = \partial\sigma^{(2)}_{zz}/\partial z = S^*(\partial^2 u^{(2)}_z/\partial z^2) + \lambda^*(\partial T_2/\partial z) \qquad (15)$$

The general solution of Eq.(15) is given by

$$u^{(2)}_z(z) = R_2(0)e^{-ik_2(z-l_1)} + S_2(0)e^{ik_2(z-l_1)} + \qquad (16)$$

$$\{\lambda^*\sigma'_2\pi/S^*[(\sigma'_2)^2 + (k_2)^2]\}\{C(0)e^{-\sigma'_2(z-l_1)} - D(0)e^{\sigma'_2(z-l_1)}\} \ .$$

If the output terminals of the PZT is open, $D_z = 0$. Thus, from Eqs.(14), (16), and (5a), we get

$$\sigma^{(2)}_{zz}(z) = -ik_2S^*[R_2(0)e^{-ik_2(z-l_1)} - S_2(0)e^{ik_2(z-l_1)}] + \qquad (14a)$$

$$\{\lambda^*(k_2)^2\pi/[(\sigma'_2)^2 + (k_2)^2]\}\{C(0)e^{-\sigma'_2(z-l_1)} + D(0)e^{\sigma'_2(z-l_1)}\} \ .$$

Using boundary conditions

$$\sigma^{(1)}_{zz}(0,t) = 0 \ , \quad \sigma^{(1)}_{zz}(l_1,t) = \sigma^{(2)}_{zz}(l_1,t) \ , \quad u^{(1)}_z(l_1,t) = u^{(2)}_z(l_1,t) \ , \quad \sigma^{(2)}_{zz}(l_1+l_2,t) = 0 \ .$$

we obtain the coefficients

$$R_2(0), S_2(0) = \{-i\gamma Yk_1{}^2Q_1e^{+ik_2l_2} + Q_2[k_2\gamma C^*\cos k_1l_1 \pm iYk_1\sin k_1l_1] + iYk_1Q_3e^{+ik_2l_2}\sin k_1l_1$$

$$\pm i\gamma Q_4e^{+ik_2l_2}\cos k_1l_1\} \ / \ 2i(Yk_1\sin k_1l_1\cos k_2l_2 - k_2\gamma S^*\cos k_1l_1\sin k_2l_2) \qquad (17)$$

where the up signs are for $R_2(0)$ and the down signs for $S_2(0)$, and

$$Q_1 = -\{\Gamma(0)e^{-\beta z_o}/(\beta^2+k_1{}^2) + [A(0) + B(0)/(\sigma_1{}^2+k_1{}^2)\} \ , \qquad \gamma = \pi\alpha_T(1+\nu)/(1-\nu)$$

$$Q_2 = [\ -i\pi\lambda^*k_2/S^*(\sigma'_2{}^2+k_2{}^2)][C(0)e^{-\sigma'_2l_2} + D(0)e^{\sigma'_2l_2}] \quad , \qquad Y = -\pi\alpha_TE/(1-2\nu)$$

$$Q_3 = \{-\pi\lambda^*\sigma'_2[C(0) - D(0)]/S^*(\sigma'_2{}^2+k_2{}^2) - \qquad (17a)$$

$$\gamma\beta\Gamma(0)e^{-\beta(l_1-z_o)}/(\beta^2+k_1{}^2) - \gamma\sigma'_1[A(0)e^{-\sigma'_1l_1} - B(0)e^{\sigma'_1l_1}]\}/(\sigma'_1{}^2+k_1{}^2)]$$

$$Q_4 = \pi\lambda^*k_2{}^2[C(0) - D(0)]/(\sigma'_2{}^2+k_2{}^2) -$$

$$Yk_1{}^2\{\Gamma(0)e^{-\beta(l_1-z_o)}/(\beta^2+k_1{}^2) - [A(0)e^{-\sigma'_1l_1} + B(0)e^{\sigma'_1l_1}]/(\sigma'_1{}^2+k_1{}^2)\} \ .$$

OUTPUT SIGNAL OF PZT

If the output terminals of the PZT are open (i.e. $D_z = o$) and the pyroelectric effect is ignored, the PZT output signal can be obtained from Eq.(13b), (16) and (17):

$$V = (e_3^T l_2 / \varepsilon_3^{ST} A_2) \int_{l_1}^{l_1+l_2} (\partial u^{(2)}_z / \partial z) dz \qquad (18)$$

$$= (e_3^T l_2 / \varepsilon_3^{ST} A_2)\{ R_2(0)(e^{-ik_2 l_2} - 1) + S_2(0)(e^{ik_2 l_2} - 1) +$$

$$[\pi\lambda^* \sigma'_2 / S^*(\sigma'^2_2 + k_2^2)][C(0)(e^{-\sigma' 2 l_2} - 1) - D(0)(e^{\sigma' 2 l_2} - 1)]$$

where A_2 is the coupling area between the sample and PZT.

Usually, the sample and PZT in SEAM are considered to be thermally thick (i.e. the linear dimensions are larger than a thermal wavelength). In this case, the output signal V can be approximated as the sum of an acoustical and a thermal wave signal as

$$V = V_{acoust} + V_{thermal} = G\Phi + V_{thermal} \qquad (18a)$$

where

$$G = k_1 \sin^2(k_2 l_2/2) / (k_1 C_{11} \sin k_1 l_1 \cos k_2 l_2 + k_2 S^* \cos k_1 l_1 \sin k_2 l_2)$$

$$\Phi = \Phi_o k_1 (1 + k_1^2/\sigma'^2_1 + \beta^2/\sigma'^2_1 - \beta/\sigma'_1) / \sigma'^2_1 \beta (1 + k_1^2/\sigma'^2)(1 + k_1^2/\beta^2)(1 - \beta/\sigma'_1) \qquad (18b)$$

$$\Phi_o = 4 e_3^T l_2 \alpha_T E \eta P_o e^{-\beta z_o} / \pi \varepsilon_3^{ST} A_2 \kappa_1 (1-2\nu), \qquad C_{11} = E(1-\nu)/(1+\nu)(1-2\nu)$$

$$V_{thermal} = \pi e_3^T l_2 \lambda_3^T \sigma'_2 \Gamma(0)[e^{-\beta(l_1 - z_o)} + 2 r_1 e^{-\beta z_o - \sigma' 1 l_1}] / \varepsilon_3^{ST} A_2 S^* (\sigma'^2_2 + k_2^2)(b_1 + 1) \qquad (19)$$

The factor G describes the purely acoustic properties of the sample - PZT system. The condition

$$\rho_1 C_1 \tan k_1 l_1 = -\rho_2 C_2 \tan k_2 l_2$$

produces system resonance where C_1 and C_2 are the longitudinal wave velocities in the sample and PZT, respectively. The factor ϕ describes the thermoelastic properties of the sample. The V_{acoust} signal detected by the transducer is thus determined by the sample thermoelastic properties but is modulated by the purely mechanical vibrational response of the sample - PZT system. There are six limiting cases of interest for this signal as shown in table 1.

Table 1. Six limiting results for factor Φ

Case	Limiting Relation	Limiting Result
1	$\beta^2 >> \lvert\sigma'_1{}^2\rvert >> k_1^2$	$-\Phi_0 k_1 / \sigma'_1{}^3$
2	$\lvert\sigma'_1{}^2\rvert >> \beta^2 >> k_1^2$	$\Phi_0 k_1 / \beta\sigma'_1{}^2$
3	$\beta^2 >> k_1^2 >> \lvert\sigma'_1{}^2\rvert$	$\Phi_0 / \sigma'_1 k_1$
4	$k_1^2 >> \beta^2 >> \lvert\sigma'_1{}^2\rvert$	$\Phi_0 / \sigma'_1 k_1$
5	$\lvert\sigma'_1{}^2\rvert >> k_1^2 >> \beta^2$	$\Phi_0 \beta / \sigma'_1{}^2 k_1$
6	$k_1^2 >> \lvert\sigma'_1{}^2\rvert >> \beta^2$	$\Phi_0 \beta / \sigma'_1{}^2 k_1$

At typical operating frequencies (0.1 - 1.0MHz) the thermal signal is small in comparison to the acoustic signal. Nonetheless $V_{thermal}$ has two limiting cases worthy of mention for transducers having a large value of λ_3^T. Usually $\lvert\sigma'_2\rvert >> k_2$ in the frequency range 0.1 - 1 MHz. Then, when $\beta >> \lvert\sigma'_1\rvert$,

$$V_{thermal} = -2e_3^T l_2 \lambda_3^T \eta P_0 e^{-\beta z_0 - \sigma'_1 l_1} / \pi\varepsilon_3^{ST} A_2 S^* \kappa_1 (b_1+1)\sigma'_1\sigma'_2 \quad . \tag{19a}$$

The signal is thus proportional to the beam power P_0 and ω^{-1}. When $\beta << \lvert\sigma'_1\rvert$,

$$V_{thermal} = e_3^T l_2 \lambda_3^T \eta \beta P_0 e^{-\beta(l_1 - z_0)} / \pi\varepsilon_3^{ST} A_2 S^* \kappa_1 (b_1+1)\sigma'_1{}^2\sigma'_2 \quad . \tag{19b}$$

In this case, the output signal is proportional to βP_0 and $\omega^{-3/2}$.

DISCUSSION AND CONCLUSION

Eq.(18) shows that an AC heat source can generate both thermal and acoustical signals. Although the thermal wave attenuates very rapidly, information about the thermoelastic properties of the irradiated
region is carried by the acoustical wave and received by the PZT. The amplitude and phase of the PZT output signal depends on the thermal, mechanical and electrical properties of the sample since

$$V_{acoust} \sim \alpha_T E / \kappa_1(1-2\nu) \ , \qquad V_{thermal} \sim \sigma'_1 / (\kappa_1\sigma'_1 + \kappa_2\sigma'_2) \ .$$

If there are variations of these parameters in the irradiated region, we will get image contrast.

The relationship between the signal and beam power P_0 has been experimentally determined[5]. When the modulating frequency is in the range 0.1 - 1MHz and the thickness l_1 of the sample is about 1 - 3 mm, the sample may be considered to be thermally thick. We may estimate β as

$$\beta = 1 / z_0 = 20\rho_1 / V_0^{1.43} \ .$$

For copper, for example, $\beta = 1.39\mu m^{-1}$ and $|\sigma'_1| = 0.08\mu m^{-1}$ when $V_0 = 30kV$ and $f = 235kHz$ (case 1 of Table 1), both V_{acoust} and $V_{thermal}$ are proportional to the beam power P_0. These findings are in agreement with the experimental results of reference [5].

ACKNOWLEDGEMENT

We express sincere thanks to Prof. A. Howie for his very useful suggestions.

REFERENCES

* Permanent address: Institute of Acoustics, Tongji University, Shanghai, People's Republic of China.

** Permanent address: NASA Langley Research Center, Hampton, Virginia 23665-5225 USA.

1. Davies D.G. 1986 Phil. Trans. R. Soc. Lond. A**320** 243

2. Brandis E. and Rosencweig A. 1980 Appl. Phys. Letts. **37** 98

3. Cargill G.S. 1980 Nature **286** 691

4. Davies D.G. Howie A. and Staveley-Smith L. 1983 J. Soc. Photo-optical Instrumentation Engineers (Washington) **368** 58

5. Rocca F.J. and Davies D.G. "Signal production in scanning Electron Acoustic Microscopy" (to be published)

6. Donolato C. and Venturi P. 1982 Phys. Stat. Sol. (a) **73** 377

7. Obmer M.C. et .al. 1988 J. Appl. Phys. **64** (5) 2775